KAVAKA 58 (2) : 5-10 (2022) DOI: 10.36460/Kavaka/58/2/2022/5-10

# Antifungal efficacy of mycosynthesized silver-selenide nanoparticles against *Aspergillus niger* and their antioxidant activity evaluation

Sk Najrul Islam, Sadia Parveen, Syed Mohd Adnan Naqvi, Azam Raza and Absar Ahmad*

*Interdisciplinary Nanotechnology Centre (INC), Z. H. College of Engineering and Technology, Aligarh Muslim University, AMU, Aligarh, UP-202 002, India*

**Corresponding author Email: aahmad786in@gmail.com*

(Submitted on March 29, 2022; Accepted on May 18, 2022)

## ABSTRACT

**The green approaches of nanoparticle synthesis using microorganisms have become a subject of great interest as microbial synthesis is highly reproducible, reliable, cheap, and can be easily up-scaled, resulting in the production of highly stable, water-dispersible nanoparticles in abundant quantities. Recently, our group has synthesized gold selenide (AuSe) nanoparticles (NPs) and studied their antisporulant activity against *Aspergillus niger*. AuSe NPs inhibit sporulation only, and not the mycelial growth of the fungus. In order to inhibit both, sporulation and mycelial growth of the *A. niger*, and find a cost-effective alternative to the much more expensive gold raw material, we concentrated our efforts on synthesizing Silver Selenide ($Ag_2Se$) NPs. Herein, the chalcogenide semiconducting $Ag_2Se$ NPs have been successfully mycosynthesized through a two-step sequential reaction using the endophytic fungus *Fusarium oxysporum*. These mycosynthesized $Ag_2Se$ NPs with an average particle size of 11 nm have been fully characterized using TEM, XRD, UV-Vis-NIR, FTIR, and Fluorescence Spectrometer, while the optical bandgap energy (2.3 eV) of $Ag_2Se$ NPs was determined by the tauc plot method. Additionally, the disc diffusion method tested the antifungal activity of these mycosynthesized NPs, and the spotted inhibition zone across the sterile discs confirmed their antifungal potency against *Aspergillus niger*. The antioxidant activity of $Ag_2Se$ NPs was evaluated using the DPPH scavenging assay with 83.3% scavenging efficiency.**

**Keywords:** $Ag_2Se$ NPs, Antifungal, Antioxidant, Endophyte, Mycosynthesis

## INTRODUCTION

Recently, semiconducting chalcogenide selenide nanoparticles have received great attention from the world scientific community due to their extensive applications in catalysis (Diko *et al.,* 2020), energy storage (Lu *et al.,* 2017), optoelectronics (Thakar and Lodha, 2019), biomedical science (Islam *et al.,* 2022), etc. Among different selenide nanoparticles, $Ag_2Se$ NPs have been identified as a promising material for their unique optical (Andal and Buvaneswari, 2015), thermo-electrical (Pei *et al.,* 2013; Chand and Sharma, 2018), and other physicochemical properties (Yang *et al.,* 2020; Ramezanloo *et al.,* 2018). The $Ag_2Se$ NPs, belonging to the $A^{I}_{2}B^{VI}$ semiconductor group, exhibit room temperature stable orthorhombic (β-$Ag_2Se$) phase which can be transformed to the cubic (α-$Ag_2Se$) phase above 133°C. Irrespective of their phases, different chemical (Liu *et al.,* 2002; Sahu *et al.,* 2014; Tan *et al.,* 2014) methods have been reported to fabricate $Ag_2Se$ NPs. Since these methods require toxic chemicals and yield agglomerated large particles due to their lesser stability, green synthesis pathways are extensively adopted for nanofabrication. Our group has a key contribution in the biosynthesis of several chalcogenide nanoparticles (Ahmad *et al.,* 2002; Ansary *et al.,* 2007; Kumar *et al.,* 2007; Syed and Ahmad, 2013; Senapati *et al.,* 2014). Recently, plant (*Melilotus officinalis*) and sugar assisted green approaches have been successfully applied for the production of $Ag_2Se$ NPs (Armijo *et al.,* 2020; Mirzaei *et al.,* 2021). As the microorganism-based nanoparticle synthesis mechanism is highly reproducible and not varied with geographical and seasonal variation, we have mycosynthesized highly stable, water dispersible, protein capped $Ag_2Se$ NPs using endophytic fungus *Fusarium oxysporum*.

Nowadays, compounds having antifungal and antioxidant activity are being used extensively in food industries and medicines (Leyva *et al.,* 2017; Scorzoni *et al.,* 2017). In the food industry, antifungal agents reduce economic losses by inhibiting the microbial spoilage of foods while antioxidant agents prevent undesirable oxidation, thereby collectively increasing products' shelf-life. On the other hand, diseases like aspergillosis and allergic disease caused by *Aspergillus* species were observed in both normal and immune-compromised hosts (Roh and Shin, 2014). Some mycotoxins (secondary metabolites) produced by filamentous fungi may have carcinogenic and mutagenic effects on humans and other animals (Mutlu-Ingok *et al.,* 2020). Thus, the scientific community is highly focused on discovering antifungal agents that inhibit the growth of mycotoxigenic fungi and reduce the effect of mycotoxins. Antifungal and antioxidant agents that can inhibit fungal growth and protect cell membranes from mycotoxins-induced damage, respectively, are of prime importance for developing new, improved drugs to control both fungal infection and mycotoxicosis.

## MATERIALS AND METHODS

### Chemicals

For the mycosynthesis of $Ag_2Se$ NPs, selenium tetrachloride ($SeCl_4$, Sigma Aldrich) and silver nitrate ($AgNO_3$, Sigma Aldrich) were used as main precursors. At the same time, D-glucose (Qualigens), agar-agar (Merck), malt extract (Himedia), yeast extract (Himedia), and peptone (Himedia) were utilized for media preparation and fungi culture. 2,2-diphenyl-1-picrylhydrazyl (DPPH) was procured from Alfa Aesar, and all the analytical reagent-grade chemicals were used as received from commercial suppliers.

### Biomass production and fungiculture

The strain of endophytic fungus *Fusarium oxysporum* was revived on potato dextrose agar (PDA) slants from the previously stoke culture (Islam *et al.,* 2021a), which was maintained by monthly sub-culturing. The freshly prepared slants were then kept under observation in the B.O.D. incubator at 25°C for 96 hours. After an actively growing culture was observed on the slanting surface, approximately 1

$cm^2$ of slant's agar having *Fusarium oxysporum* was transferred into 500 ml each Erlenmeyer flasks containing 100 ml aqueous MGYP medium composed of malt extract (0.3%), glucose (1%), yeast extract (0.3%), and peptone (0.1%). These Erlenmeyer flasks were then placed on a rotary shaker (200 rpm) at 25°C. After 96h of fermentation, mycelial mass was separated from submerged culture by centrifugation (7000 rpm) at 15°C for 20 min. Then mycelia were washed thrice with sterile double distilled water under sterile conditions and applied for biosynthesis experiments.

**Mycosynthesis of $Ag_2Se$ NPs**

Herein, a two-step biosynthesis approach was employed for the mycosynthesis of $Ag_2Se$ NPs. In the first step of sequential reactions, 20g of washed biomass (*Fusarium oxysporum*) was resuspended into a 500 ml Erlenmeyer flask containing 100 ml aqueous solution of $SeCl_4$ (1 mM). After 24 h of reaction completion on a rotary shaker (200 rpm) at 25°C, the fungal biomass was filtered out from the reaction mixture by simple Whatman paper filtration. The obtained red filtrate was stored at room temperature. Finally, 50 ml of the red filtrate was mixed with a 50 ml aqueous solution of $AgNO_3$ (2 mM), and the reaction was allowed to complete without stirring. The resultant gray solution was then lyophilized and stored as a powder for further experimental studies.

**Characterization techniques**

The different characterization tools and sophisticated techniques were employed to confirm the formation of $Ag_2Se$ NPs. The light absorption properties and fluorescent behavior of these semiconductor NPs were determined using the UV-Vis-NIR spectrophotometer (Carry 5000) and Fluorescence spectrometer (Perkin Elmer), while the bandgap energy was calculated by the tauc plot method. Most importantly, Transmission Electron Microscopy (TEM, JEM-JEOL, Japan) and X-ray powder diffractometer (XRD, Rigaku) were performed to investigate the shape, size, particles size distribution, and structural parameters of the mycosynthesized $Ag_2Se$ NPs. To analyze the fundamental bond vibration in $Ag_2Se$ NPs and capping biomolecules, the FTIR spectrum was recorded using a Perkin Elmer spectrometer.

**Antifungal activity**

For testing antifungal activity of mycosynthesized $Ag_2Se$ NPs, the fungus *Aspergillus niger* was cultured on an agar medium in a test tube (slant) followed by the preparation of spore suspension by transferring $1cm^2$ of agar plugs into double distilled water. The aqueous solution of $Ag_2Se$ NPs having a concentration of 5 mg/ml and 4 mg/ml were prepared. In this disk diffusion method, spore suspension of *Aspergillus niger* was overlaid on the surface of sterile PDA plates and incubated in a BOD incubator at 25°C for initial germination. After a few hours, sterile discs were placed on the surface of PDA, and 30 µl of the test samples were loaded onto the discs (A=125 µg, B=100 µg) while sterile double distilled water was used as a negative control. The potency of antifungal activity was determined by investigating the zone of inhibition after 24, 48, and 72 h of incubation.

**Antioxidant activity**

The antioxidant activity of the mycosynthesized $Ag_2Se$ NPs was determined by reducing the radical 2, 2-diphenyl-1-picrylhydrazyl (DPPH) (Islam *et al.,* 2021b). Initially, the standard methanolic solution of DPPH (0.01 mM) and various concentrated (100-1000 µg/ml) aqueous $Ag_2Se$ NPs was prepared. Then, 2 ml of DPPH solution was mixed with 1 ml of different concentrations of NP solutions separately and incubated for 10 min in darkness. After 10 min of incubation, the absorbance of all the aliquots was measured whereas methanolic DPPH without NPs and methanol served as control and blank, respectively. The percentage of DPPH scavenging was calculated using the following formula

$$\%\ Scavenging = \frac{Abs\ (c) - Abs(s)}{Abs\ (c)} \times 100$$

Where Abs (c) and Abs (s) represent absorbance of control and sample absorbance respectively.

**RESULTS AND DISCUSSION**

The biofabrication of $Ag_2Se$ NPs was monitored by recording the UV-Vis spectrum (**Fig. 1a**) in the wavelength range of 350

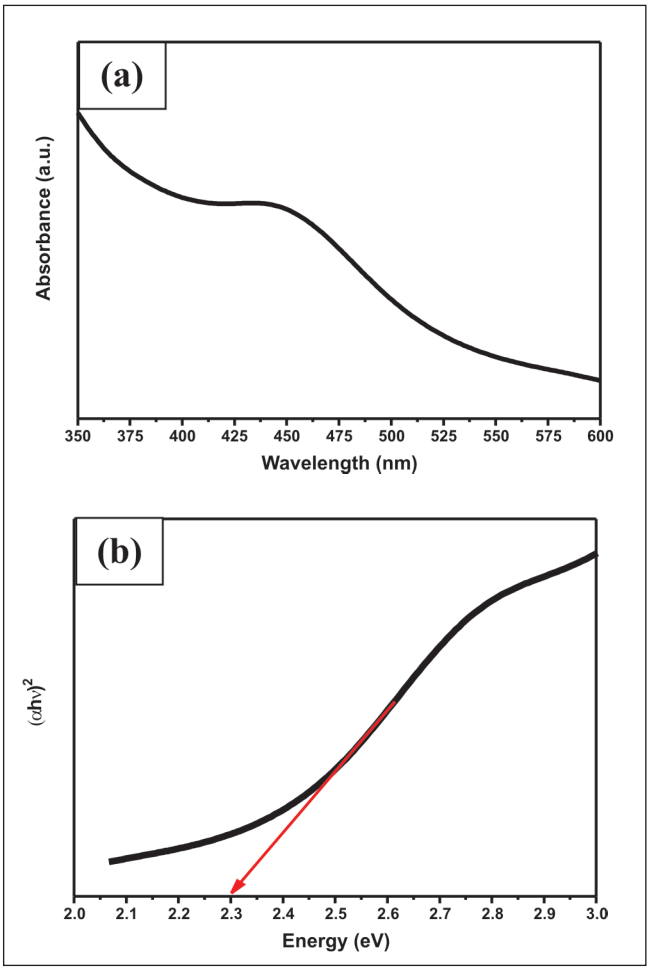



**Fig. 1:** UV-Visible spectrum (a) and tauc plot (b) of mycosynthesized $Ag_2Se$ nanoparticles

to 600 nm. The recorded spectrum (**Fig. 1a**) showed a broad absorption peak between 420 and 460 nm with an absorption maxima of 440 nm. The change in colour of the reaction mixture from red to gray during the sequential reduction of $SeCl_4$ and $AgNO_3$ salts and the observed characteristic absorption band at 440 nm initially confirmed the formation of $Ag_2Se$ NPs (Armijo *et al.,* 2020; Mirzaei *et al.,* 2021). The shifting in absorption maxima from 413 nm (reported) to 440 nm can be attributed to the surface capping of the $Ag_2Se$ NPs by the fungus secreted protein molecules (Armijo *et al.,* 2020).

As the tauc method was extensively used to determine the optical bandgap of semiconductor materials, the bandgap energy of $Ag_2Se$ semiconductor NPs was evaluated using the tauc plot (**Fig. 1b**) and was found to be 2.3 eV (Gnanadurai *et al.,* 2018; Armijo *et al.,* 2020).

The optical characterization of mycosynthesized $Ag_2Se$ NPs was accomplished by recording the PL emission spectrum (**Fig. 2**) corresponding to the excitation wavelength of 375 nm. The spectrum showed an intense emission peak at 430 nm which is the characteristic emission band edge of $Ag_2Se$ NPs, confirming the formation of $Ag_2Se$ NPs (More *et al.,* 2016).

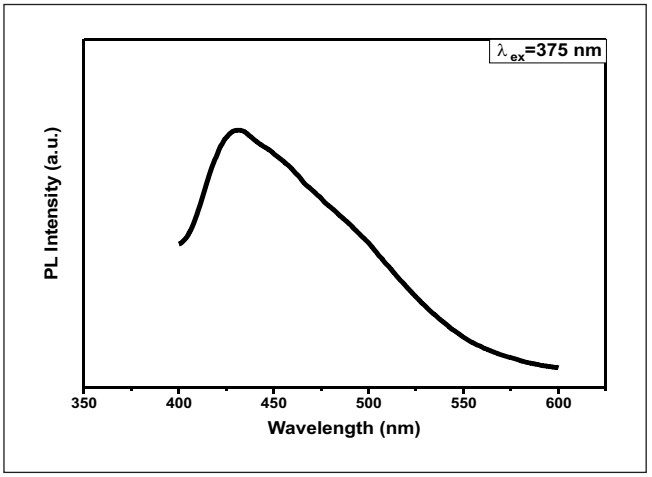



**Fig. 2:** PL emission spectrum of mycosynthesized $Ag_2Se$ nanoparticles.

After the completion of sequential reactions followed by the investigation of optical properties, the mycosynthesized $Ag_2Se$ NPs were subjected to TEM analysis to estimate their shape, average size, and particle size distribution. The TEM micrographs (**Fig. 3a, b**) and the particle size distribution histogram (**Fig. 3c**) displayed that the mycosynthesized $Ag_2Se$ NPs are spherical in shape with an average particle diameter of 11 nm.

The X-ray diffractograms of a synthesized (lyophilized powder) $Ag_2Se$ NPs and calcined $Ag_2Se$ NPs were shown in **Fig. 4a**. The broad diffraction peaks originating at the 2θ angle of 30.9°, 33.5°, 36.9°, 51.6°, 54.9° and 63.7° correspond to the crystallographic planes of (102), (112), (013), (104), (222) and (043) for mycosynthesized $Ag_2Se$ NPs, match well with the standard diffractogram of orthorhombic $Ag_2Se$ (JCPDS, 00-024-1041). In addition, the sharpness and minor shifting of the diffraction peaks for annealed $Ag_2Se$ NPs were observed due to the thermal aggregation of NPs and the desorption of protein molecules by heating.

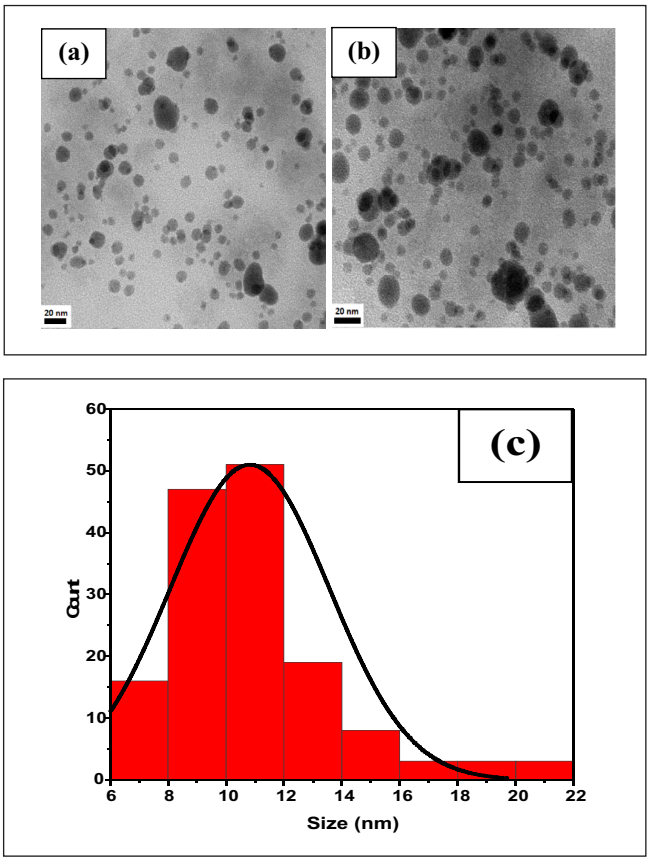



**Fig. 3.** TEM micrographs (a, b) and particle size distribution histogram (c) of mycosynthesized $Ag_2Se$ nanoparticles

FTIR spectroscopy is a well-known analytical technique that was wildly used to determine the fundamental bond vibration frequency of biosynthesized NPs and their interaction with capping biomolecules. The FTIR spectrum of mycosynthesized $Ag_2Se$ NPs was recorded in the wavenumber range of 800-2400 $cm^{-1}$ and is shown in **Fig. 4b**. The spectrum showed two characteristic absorptions at 1384 $cm^{-1}$ and 1407 $cm^{-1}$ corresponding to stretching vibration of Ag–Se bond (Chougale *et al.,* 2013; Mirzaei *et al.,* 2021) while the absorption band appearing at 1632 $cm^{-1}$ was characterized for stretching vibration of N–C=O (amide (I) band) associated with the capping protein molecules (Islam *et al.,* 2021c).

**Antifungal and antioxidant activity of $Ag_2Se$ NPs**

The antifungal activity of mycosynthesized $Ag_2Se$ NPs was evaluated against *Aspergillus niger* after the incubation time of 24, 48, and 72 h (**Fig. 5**). The strong antifungal efficacy of the mycosynthesized $Ag_2Se$ NPs was confirmed by the zones

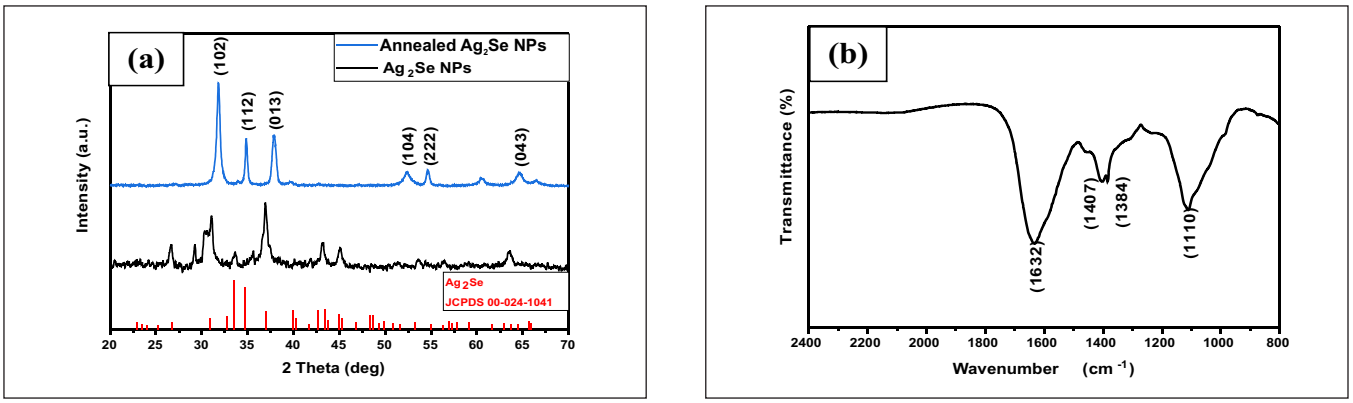



**Fig. 4:** (a) XRD pattern and (b) FTIR spectrum of mycosynthesized $Ag_2Se$ NPs

of inhibition which were encircled across the sterile disks containing Nps. It was also observed that the inhibition zone diameter for 125 µg dose is greater than 100 µg while no zone of inhibition was observed for $H_2O$.

The DPPH scavenging efficacy of $Ag_2Se$ NPs was investigated by assessing UV-vis absorbance spectra at a wavelength of 517 nm. The absorbance of DPPH was decreases with increasing of $Ag_2Se$ NPs concentration (A1= 62.5 µg/ml, A2= 125 µg/ml, A3= 250 µg/ml, A4= 500 µg/ml and A5= 1000 µg/ml) revealed good antioxidant potency of the mycosynthesized $Ag_2Se$ NPs (**Fig. 6a**). These NPs show 88.3% scavenging efficiency within the 5 min of NPs addition (1000 µg/ml) (**Fig. 6b**)

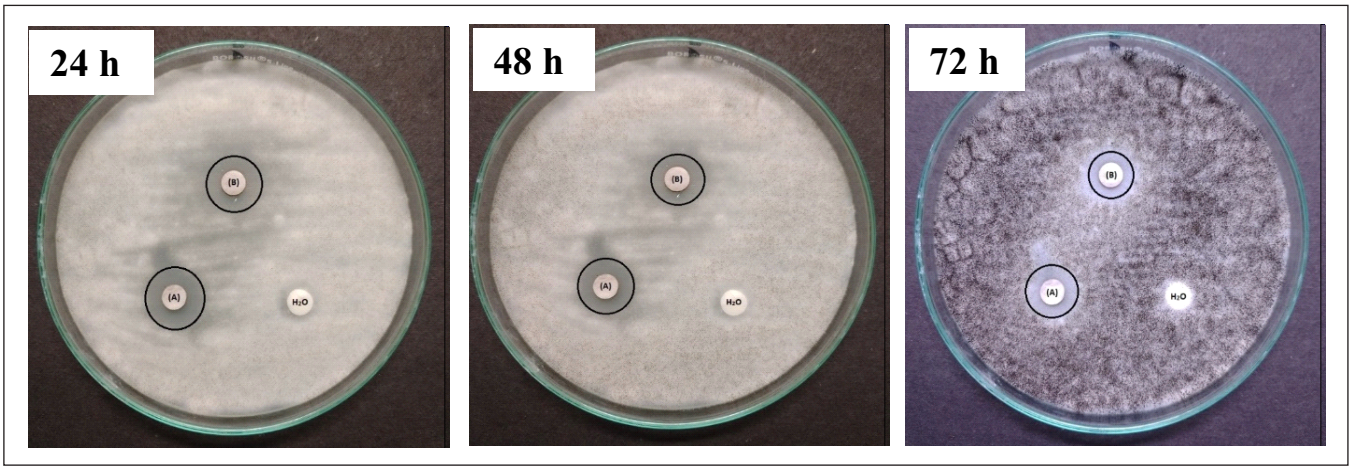



**Fig. 5:** Antifungal activity of mycosynthesized $Ag_2Se$ nanoparticles against *Aspergillus niger*

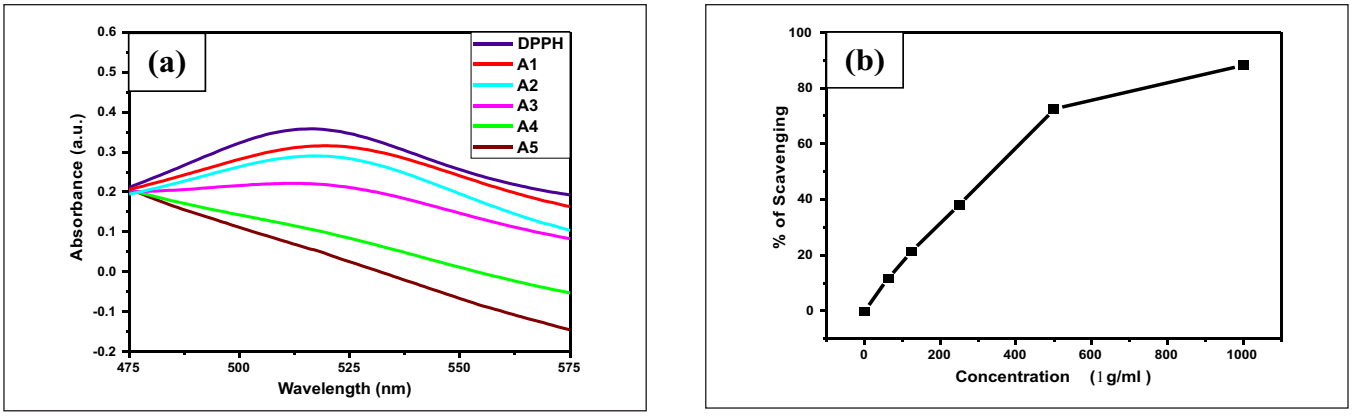



**Fig. 6:** (a) The UV-Vis spectra of DPPH with increasing concentration of $Ag_2Se$ NPs. (b) Concentration-dependent scavenging efficacy

## CONCLUSION

The present investigation demonstrated the use of endophytic fungus *Fusarium oxysporum* for the mycosynthesis of $Ag_2Se$ NPs at room temperature via a simple, cost-effective,

sequential two-step reaction. These semiconducting mycosynthesized protein capped $Ag_2Se$ NPs with an average particle size of 11 nm (TEM) showed bandgap energy of 2.3 eV. The stable crystalline orthorhombic phase (β-$Ag_2Se$) of these NPs has been determined by XRD measurement. Additionally, the antioxidant activity of these $Ag_2Se$ NPs was evaluated by DPPH assay with 88.3% scavenging efficiency, and strong antifungal activity was obtained against *Aspergillus niger*. When fungal drug resistance and mycotoxicosis are increasing to a new higher level, our mycosynthesized $Ag_2Se$ NPs exhibiting antifungal and antioxidant activity may play an essential role in developing new, improved drugs at extremely cost-efficient means and abundant quantities.

## ACKNOWLEDGMENTS

We acknowledge the Department of Biotechnology (DBT), Government of India, for setting up a Centre of Excellence (COE, BT/PR1-3584/COE/34/29/2015) at the Inter-disciplinary Nanotechnology Centre (INC), Aligarh Muslim University, AMU, Aligarh, UP-202002, India. We thank Mr. Ashraf Ali Khan and Mr. Alim Kazmi of INC for their technical assistance.

## REFERENCES

Ahmad, A., Mukherjee, P., Mandal, D *et al.* 2002. Enzyme mediated extracellular synthesis of CdS nano-particles by the fungus, *Fusarium oxysporum*. *J. Am. Chem. Soc.* **124:** 12108-12109.

Andal, V. and Buvaneswari, G. 2015. Effect of nature of surfactant on the formation of β-$Ag_2Se$ nano-particles and optical properties of β-$Ag_2Se$ and ZnS/β-$Ag_2Se$ nanocomposite. *J. Nano Res.* **30:** 96-105.

Ansary, A.A., Kumar, S.A., Krishnasastry, M.V. *et al.* 2007. CdS quantum dots: Enzyme mediated *in vitro* synthesis, characterization and conjugation with plant lectins. *J. Biomed. Nanotechnol.* **3:** 406-413.

Armijo, D., Mendoza, L., Vizuete, K. *et al.* 2020. Sugar-mediated green synthesis of silver selenide. *Molecules* **25:** 1-18.

Chand, S. and Sharma, P. 2018. Synthesis and characterization of Ag-chalcogenide nanoparticles for possible applications in photovoltaics. *Mater. Sci. Pol.* **36:** 375-380.

Chougale, U.M., Han, S.H., Rath, M.C. *et al.* 2013. Synthesis, characterization and surface deformation study of nanocrystalline $Ag_2Se$ thin films. *Mater. Phys. Mech.* **17:** 47-58.

Diko, C.S., Qu, Y., Henglin, Z. *et al.* 2020. Biosynthesis and characterization of lead selenide semiconductor nanoparticles (PbSe NPs) and its antioxidant and photocatalytic activity. *Arab J. Chem.* **13:** 8411-8423.

Gnanadurai, P., Maheshwaran, A. and Velvizhi, R. 2018. Synthesis and characterization of silver selenide ($Ag_2Se$) nanoparticles. *Journal of Analysis and Computation (JAC)*. **XI:** 1-10.

Islam, S.N., Raza, A., Naqvi, S.M.A. *et al.* 2022. Unveiling the antisporulant activity of mycosynthesized gold-selenide nanoparticles against black fungus *Aspergillus niger*. *Surfaces and Interfaces* **29:** 101-769.

Islam, S.N., Naqvi, S.M.A., Parveen, S. *et al.* 2021a. Application of mycogenic silver/silver oxide nanoparticles in electrochemical glucose sensing ; alongside their catalytic and antimicrobial activity. *3 Biotech* **11:** 3-42.

Islam, S.N., Naqvi, S.M.A., Parveen, S. *et al.* 2021b. Effect of Endophytic Fungus *Fusarium oxysporum* on Crystallographic Properties of PdO : Nanoparticles Synthesis, Characterization and Evaluation of Antioxidant Activity. In: *International Conference on Evolving Materials and Nanotechnology for Sustainable Development (EMNSD)*: 136-146.

Islam, S.N., Naqvi, S.M.A., Parveen, S. *et al.* 2021c. Endophytic fungus-assisted biosynthesis, characterization and solar photocatalytic activity evaluation of nitrogen-doped $Co_3O_4$ nanoparticles. *Appl. Nanosci.* **11(5):** 1651-1659.

Kumar, S.A., Ansary, A.A., Abroad. A. *et al.* 2007. Extracellular biosynthesis of CdSe quantum dots by the fungus, *Fusarium oxysporum*. *J. Biomed. Nanotechnol* **3:** 190-194.

Leyva S.M., Mounier, J., Valence, F. *et al.* 2017. Antifungal microbial agents for food biopreservation: a review. *Microorganisms* **5:** 1-35.

Liu, S.H., Qian, X.F., Yin, J. *et al.* 2002. Synthesis and characterization of $Ag_2S$ nanocrystals in hyperbranched polyurethane at room temperature. *J. Solid State Chem.* **168:** 259-262.

Lu, T., Dong, S., Zhang, C. *et al.* 2017. Fabrication of transition metal selenides and their applications in energy storage. *Coord. Chem. Rev.* **332:** 75-99.

Mirzaei, S.Z., Lashgarian, H.E., Karkhane, M. *et al.* 2021. Bio-inspired silver selenide nano-chalcogens using aqueous extract of *Melilotus officinalis* with biological activities. *Bioresour. Bioprocess* **8:** 5-6.

More, D.S., Moloto, M.J. and Moloto, N. 2016. Hexadecylamine capped silver selenide nano-particles : Temperature study. *Chalcogenide Letters* **13:** 233-238.

Mutlu-Ingok, A., Devecioglu, D., Dikmetas, D.N. *et al.* 2020. Antibacterial, antifungal, antimycotoxigenic, and

antioxidant activities of essential oils: An updated review. *Molecules* **25:** 4711.

Pei, J., Chen, G.,Jia, D. *et al.* 2013. Rapid synthesis of $Ag_2Se$ dendrites with enhanced electrical performance by microwave-assisted solution method. *New J. Chem.* **37:** 3-23.

Ramezanloo, B., Molaei, M. and Karimipour. M. 2018. Red emissive $Ag_2Se$ quantum dots (QDs) with room-temperature synthesis of both orthorhombic and superionic cubic phases via stirring approach. *J. Lumin.* **204:** 419-423.

Roh, J and Shin, S. 2014. Antifungal and antioxidant activities of the essential oil from *Angelica koreana* Nakai. *Evidence-based Complement*. *Altern. Med.* **2014:** 398-503.

Sahu, A., Braga, D., Waser, O. *et al.* 2014. Solid-phase flexibility in $Ag_2Se$ semiconductor nanocrystals. *Nano. Lett.* **14(1):** 115-121.

Scorzoni, L., de Paula e Silva, A.C.A., Marcos, C.M. *et al.* 2017. Antifungal therapy: New advances in the understanding and treatment of mycosis. *Front. Microbiol.* **8:** 36.

Senapati, S., Syed, A., Khan, S. *et al.* 2014. Extracellular biosynthesis of metal sulfide nanoparticles using the fungus *Fusarium oxysporum*. *Curr. Nanosci.* **10:** 588-595.

Syed, A. and Ahmad, A. 2013. Extracellular biosynthesis of CdTe quantum dots by the fungus *Fusarium oxysporum* and their anti-bacterial activity. *Spectrochim Acta-Part A Mol. Biomol. Spectrosc.* **106:** 41-47.

Tan, L., Fu, J. and Liu, S. 2014. Growth of photoluminescent $Ag_2Se$ nanowires from a simple precursor solution. *Cryst. Eng. Comm.* **16:** 10534-10538.

Thakar, K. and Lodha, S. 2019. Optoelectronic and photonic devices based on transition metal dichalcogenides. *Mater. Res. Express.* **7:** 014002.

Yang, X., Wang, C., Zhang, X. *et al.* 2020. Photothermal and adsorption effects of silver selenide nanoparticles modified by different surfactants in nursing care of cancer patients. *Science and Technology of Advanced Materials* **21(1):** 584-592.